The EMBO Journal Vol.16 No.21 pp.6337–6345, 1997

Carboxy-terminal domain mediates assembly of the voltage-gated rat ether-à-go-go potassium channel

Jost Ludwig, David Owen[1] and Olaf Pongs[2]

Zentrum für Molekulare Neurobiologie der Universität Hamburg, Institut für Neurale Signalverarbeitung, Martinistrasse 52, D-20246 Hamburg, Germany and [1]Department of Pharmacology, University College London, Gower Street, London WC1E 6BT, UK

[2]Corresponding author
e-mail: pointuri@uke.uni-hamburg.de

The specific assembly of subunits to oligomers is an important prerequisite for producing functional potassium channels. We have studied the assembly of voltage-gated rat ether-à-go-go (r-eag) potassium channels with two complementary assays. In protein overlay binding experiments it was shown that a 41-amino-acid domain, close to the r-eag subunit carboxy-terminus, is important for r-eag subunit interaction. In an *in vitro* expression system it was demonstrated that r-eag subunits lacking this assembly domain cannot form functional potassium channels. Also, a ~10-fold molar excess of the r-eag carboxy-terminus inhibited in co-expression experiments the formation of functional r-eag channels. When the r-eag carboxy-terminal assembly domain had been mutated, the dominant-negative effect of the r-eag carboxy-terminus on r-eag channel expression was abolished. The results demonstrate that a carboxy-terminal assembly domain is essential for functional r-eag potassium channel expression, in contrast to the one of Shaker-related potassium channels, which is directed by an amino-terminal assembly domain.

Keywords: K^+ current/potassium channel/subunit assembly/*Shaker*

Introduction

Voltage-gated potassium (Kv) channels play an important role in controlling resting membrane potential in neuronal as well as in non-neuronal cells. In excitable cells of the nervous system they are not only responsible for repolarization of action potentials, but also for modulating their form and frequency (Hille, 1992); Kv channels are therefore an important factor in neuronal signal transmission and processing.

Kv channels in the *Shaker* family, consist of four identical or homologous α subunits (MacKinnon, 1991; Liman *et al.*, 1992) and may have four additional modulatory β-subunits (Rehm and Lazdunski, 1988; Parcej and Dolly, 1989; Parcej *et al.*, 1992; Rettig *et al.*, 1994). Each α-subunit is characterized by six putative transmembrane segments (S1–S6), with the region that is mainly responsible for forming the ion-conducting pore (H5) located between S5 and S6. The assembly of Kv channel α-subunits is primarily mediated by a region within the intracellular amino-terminus known as the tetramerization domain (T1-domain; Li *et al.*, 1992; Shen *et al.*, 1993; Deal *et al.*, 1994; Hopkins *et al.*, 1994; Shen and Pfaffinger, 1995; Xu *et al.*, 1995). This domain also confers subfamily specificity upon heteromultimeric assembly of K-channels. Furthermore, the same region has also shown to be involved in binding of β-subunits to α-subunits (Sewing *et al.*, 1996; Yu *et al.*, 1996).

In the ether-à-go-go (eag) family of channels, the subunits probably share the same structural features as Shaker-type channels (i.e. six putative transmembrane regions per subunit, and an H5 region), but the overall sequence similarity between eag and Shaker-type channels is quite low except for the H5 region. A much higher degree of homology is found between eag-type channels and inwardly rectifying K-channels (AKT1, KAT1) from plants (Anderson *et al.*, 1992; Sentenac *et al.*, 1992) and also between eag-type channels and the non-selective cyclic nucleotide-gated (cng) cation channels. In addition, eag channels have a region of yet unknown function within the C-terminus which is homologous to the cyclic nucleotide-binding domain of cng channels. It is presumed that eag-type channels consist of tetramers as the related cng family of ion channels (Kaupp *et al.*, 1989; Liu *et al.*, 1996). However, in contrast to Shaker-type channels, it is not yet known which protein domains are involved in the assembly of functional cng, AKT or eag channels.

In order to address this question, in the present study we have used a member of the eag-family, rat eag (r-eag) to study the interaction between subunits. Our approach combined the complementary techniques of a protein overlay assay and functional expression of r-eag-mediated ionic currents in a heterologous mammalian expression system. Our results provide evidence that, in contrast to Kv channels in which an N-terminal domain (T1) is crucial for assembly, r-eag assembly is mediated by a C-terminal domain.

Results

r-eag carboxy-terminus suppresses expression of r-eag-mediated current

It has been shown that the α-subunits of Shaker-type Kv channels contain within the cytoplasmic amino-terminus a domain required for tetramerization and α-subunit assembly. Co-expression of this domain, i.e. the amino-terminus, with wild-type (wt) Shaker subunits in *Xenopus* oocytes suppressed the formation of functional Kv channels (Li *et al.*, 1992). Most likely, the amino-terminus interfered with the assembly of wild-type subunits. In a first functional screen for possible assembly domains of r-eag subunits, we tested whether formation of functional r-eag channels could be suppressed by co-injection of wt

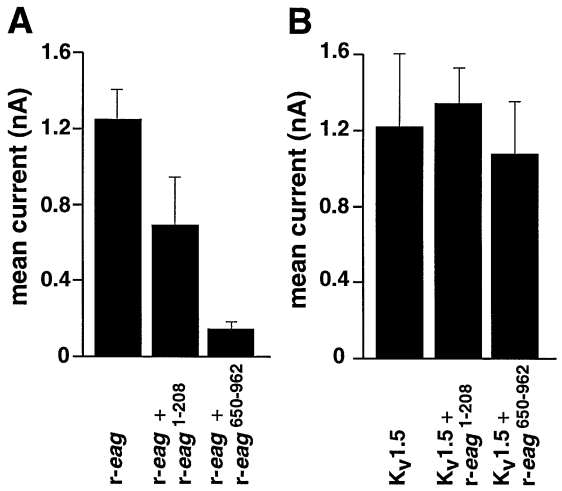

Fig. 1. Co-expression of r-eag subunits with a carboxy-terminal r-eag fragment suppresses functional expression of r-eag currents. (**A**) Data pooled from a number of experiments in which mRNAs encoding either r-eag, r-eag plus an amino-terminal fragment (r-eag$^{1–208}$) or r-eag plus a carboxy-terminal fragment (r-eag$^{650–962}$) was injected into CHO cells. Currents were recorded after 4 h and peak amplitudes were measured following a 500 ms voltage step to +60 mV. The histogram represents the mean of measurements from between 9 and 18 different cells; vertical bars represent the SEM in each case. The difference between the mean amplitudes of currents recorded following co-injection of r-*eag* with r-*eag*$^{650–962}$ (right) and r-*eag* mRNA alone (left) is highly significant ($P < 0.001$), whereas the difference between the mean of currents measured after co-injection of r-*eag*$^{1–208}$ with r-*eag* and that measured for r-*eag* mRNA alone (middle) is not statistically significant ($P > 0.05$) (Statistical analysis using Student's *t*-test). (**B**) Experiments carried out as in (A) except that Kv1.5 mRNA was injected alone or with r-*eag*$^{1–208}$ and r-*eag*$^{650–962}$ mRNA. Descriptions of the histogram and vertical bars are as for (A). Means were derived from between three and six cells. There was no statistically significant difference between any of the columns (Student's *t*-test).

r-*eag* mRNA with mRNA encoding the amino- (r-eag$^{1–208}$) or carboxy-terminal (r-*eag*$^{650–962}$) part of the r-eag protein.

Microinjection of r-*eag* mRNA into Chinese hamster ovary (CHO) cells resulted in the expression of a delayed-rectifier type voltage-gated K^+ current. Currents were recorded in whole-cell patch–clamp mode between 1 and 14 h after injection of r-*eag* RNA and on average the peak current amplitudes reached a maximum between 4 and 8 h. Between these times, the current was seen in >90% of the injected cells and at +60 mV averaged 1.24 ± 0.16 nA ($n = 18$). Typically for r-eag currents, the rate of activation was slowed dramatically from hyperpolarized holding potentials. The properties of r-eag-mediated currents in the CHO expression system were as previously described for r-eag currents when expressed in *Xenopus* oocytes or in 293 cells (Ludwig *et al.*, 1994; Stansfeld *et al.*, 1996; Terlau *et al.*, 1996).

Co-injection of r-*eag*$^{1–208}$ with r-*eag* wt RNA (in a 10:1 molar ratio) led to a small suppression of r-*eag* currents (current mean at + 60 mV: 0.69 ± 0.25 nA, $n = 9$) (Figure 1A) that was not statistically significant ($P > 0.05$). In contrast, the co-injection of r-*eag*$^{650–962}$ with r-*eag* RNA (1:1 molar ratio) resulted in a partial suppression of r-eag current (not shown). When the r-*eag*$^{650–962}$ RNA was injected in a 10-fold molar excess, virtually complete suppression of the current was observed (mean current at +60 mV: 0.13 ± 0.04 nA, $n = 18$) (Figure 1A). To rule out the possibility that the suppression of current is due to a non-specific binding of the r-eag$^{650–962}$ fragment to membrane proteins or due to saturation of intracellular protein synthesis or trafficking pathways, we used the expression of a distantly related Kv channel (Kv 1.5) as a control. Kv1.5 RNA was co-injected with a 10-fold molar excess of r-*eag*$^{1–208}$ or r-*eag*$^{650–962}$ RNA. Neither of these significantly reduced Kv1.5 currents (Figure 1B). Mean current amplitudes were 1.21 ± 0.39 nA at +60 mV ($n = 3$) for Kv1.5 alone compared with 1.33 ± 0.19 nA ($n = 5$) and 1.07 ± 0.27 nA ($n = 6$) for Kv1.5 plus r-eag$^{1–208}$ and r-eag$^{650–962}$, respectively.

Functional r-eag expression abolished by carboxy-terminal deletions

The results shown in Figure 1 suggested that the co-expression of r-eag subunits with the carboxy-terminus of r-eag suppressed the expression of r-eag-mediated current. Also, it has been shown that the heterologous expression of an amino-terminally truncated r-eag construct, lacking the first 190 aa residues, produces functional r-eag channels (Terlau *et al.*, 1997). Thus, we hypothesized that the carboxy-terminus of r-eag subunits contains sequences important for the formation of functional r-eag channels. Accordingly, we investigated the ability of carboxy-terminal deletion mutants to form functional r-eag channels in the CHO expression system. Injection of RNA corresponding to r-eag$^{1–937}$and r-eag$^{1–915}$ led to the expression of functional channels with characteristics and mean currents that were similar to wild-type (Figure 2A–C, E). This indicated that the 47 carboxy-terminal amino acid residues of r-eag protein, which were deleted in r-eag$^{1–915}$, are not essential for functional r-eag expression in CHO cells. However, deletion of the r-eag carboxy-terminus by a further 10 amino acids (r-eag$^{1–905}$), gave rise to functional channels in only three out of 22 injected cells. The mean of those currents observed was 1.57 ± 0.4 nA at +60 mV which was not significantly different from wild-type currents. No currents were observed following injection of RNA encoding r-eag$^{1–896}$ ($n = 5$) and r-eag$^{1–873}$ ($n = 5$) (Figure 2D and E). The results indicated that r-eag subunits may contain, in the vicinity of amino acid residue 905, domains(s) critical for the expression of functional r-eag channels in CHO cells.

Characterization of carboxy-terminal assembly domain in r-eag subunits

Next, we expressed fusion protein constructs (Figure 3A) of maltose binding protein (Mal) and r-eag (^{Mal}r-eag) in *Escherichia coli* (see Materials and methods). The bacterial lysates containing ^{Mal}r-eag protein constructs were separated on SDS–PAGE (Figure 3B) and blotted onto nitrocellulose membranes for protein overlay binding assays with ^{35}S-labelled r-eag ([^{35}S]r-eag) (Figure 3C) or [^{35}S]r-eag$^{1–208}$ (Figure 3D) as probe. [^{35}S]r-eag strongly interacted with ^{Mal}r-eag, ^{Mal}r-eag$^{272–962}$, ^{Mal}r-eag$^{384–962}$, ^{Mal}r-eag$^{482–962}$ and ^{Mal}r-eag$^{650–937}$; weaker binding was observed with ^{Mal}r-eag$^{650–929}$; and no interaction was visible with ^{Mal}r-eag $^{650–915}$. The [^{35}S]r-eag probe, which contained only amino-terminal residues 1–208 ([^{35}S]r-eag$^{1–208}$), did not bind to the ^{Mal}r-eag fusion proteins (Figure 3D), whereas the complementary probe [^{35}S]r-eag$^{191–962}$ interacted with the ^{Mal}r-eag fusion proteins

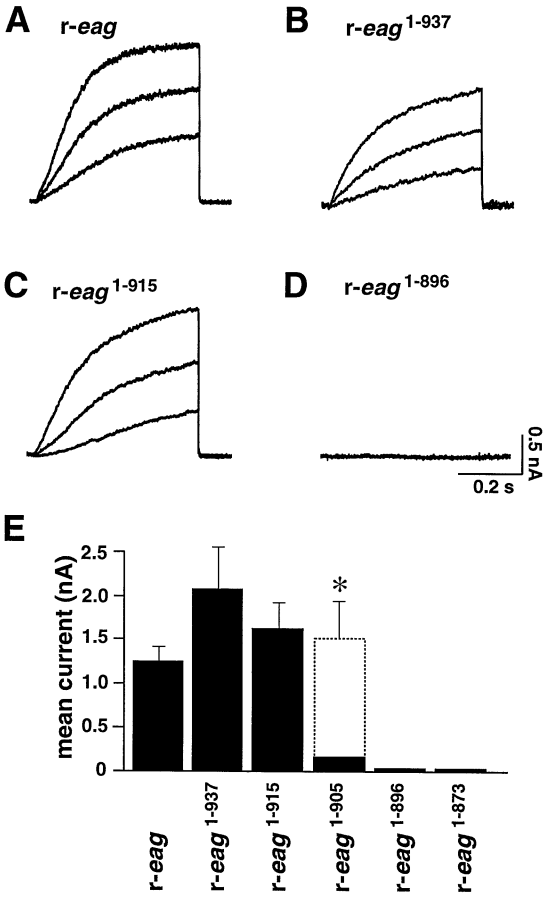

Fig. 2. Effect of carboxy-terminal deletions on expression of r-eag currents in CHO cells. Currents measured after injection of mRNA encoding r-eag (**A**), r-eag$^{1–937}$ (**B**), r-eag$^{1–915}$ (**C**) and r-eag$^{1–896}$ (**D**). In each case, currents were evoked with voltage jumps to 0 mV, +30 mV and +60 mV from a holding potential of –60 mV (traces shown superimposed). (**E**) Data pooled from a number of cells (3–18) including the constructs illustrated in (A–D) and in addition carboxy-terminal deletions r-eag$^{1–905}$ and r-eag$^{1–873}$. * indicates that r-eag$^{1–905}$ was expressed in only three of 22 cells injected.

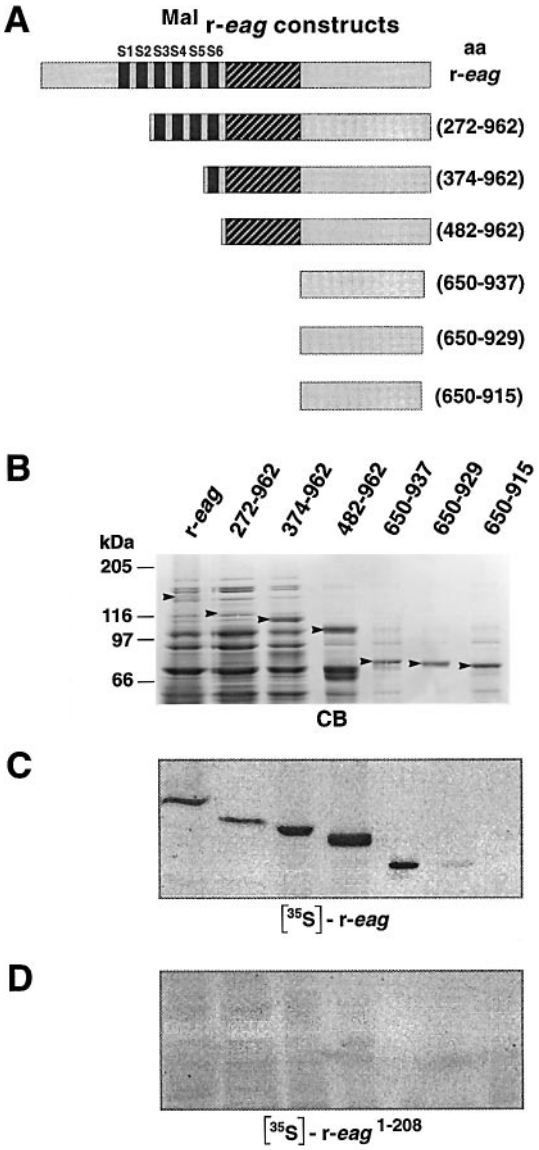

Fig. 3. Truncated r-eag proteins bind [^{35}S]r-eag, but not [^{35}S]r-eag amino-terminus. (**A**) Diagram illustrating fusion protein constructs between maltose binding protein and truncated r-eag proteins (^{Mal}r-eag) used in the overlay protein binding assays. Numbers for first and last r-eag residues (aa) in the fusion proteins are given on the right. Full-length r-eag protein (1–962) is shown on top. Black boxes indicate the putative transmembrane regions S1–S6; hatched boxes indicate the region that exhibits high similarity to the cyclic nucleotide binding domain of cyclic nucleotide-gated channels. (**B**) Coomassie blue (CB) stained SDS–polyacrylamide gel of total bacterial lysates from *E.coli* expressing the ^{Mal}r-eag fusion protein constructs shown in (A). Expression of shorter ^{Mal}r-eag constructs (^{Mal}r-eag$^{650–937}$, ^{Mal}r-eag$^{650–929}$, ^{Mal}r-eag$^{650–915}$) was more efficient than the one of the longer ^{Mal}r-eag constructs. Accordingly, the amount of bacterial protein was adjusted to load comparable amounts of ^{Mal}r-eag fusion protein. The positions of molecular weight markers (kDa) are indicated on the left. Fusion protein bands are marked by arrows. (**C** and **D**) The blots were incubated with *in vitro*-translated ^{35}S-labelled r-eag protein ([^{35}S]r-eag) (C) or r-eag amino-terminus ([^{35}S]r-eag$^{1–208}$) (D). Bound r-eag protein was visualized by autoradiography.

(see Figure 4). The data showed that amino-terminal cytoplasmic domains were not required for r-eag subunit interaction in the overlay binding experiments and that r-eag domain(s) between residues 650 and 937 were sufficient for r-eag subunit interaction. The results of the overlay binding experiments strongly supported our interpretation of the functional r-eag expression studies in Figures 1 and 2. Namely, the carboxy-terminus of r-eag subunits contains in the vicinity of amino acid residues 905 important domain(s) for r-eag subunit assembly.

To define the approximate amino-terminal border of the r-eag subunit interaction recognition domain(s) more precisely, we generated protein blots with ^{Mal}r-eag fusion protein constructs in which part of the r-eag carboxy-terminus (residues 650–937) was further truncated from its amino- and carboxy-terminal end (Figure 4A). The blots were probed with [^{35}S]r-eag$^{191–962}$ (Figure 4B and C). When the carboxy-terminus had progressively been shortened from residue 650 to residue 897, only a gradual and relatively small reduction in the intensity of the binding signal was observed. However, when further amino acids had been deleted, as in the case of the ^{Mal}r-eag$^{906–937}$ fusion protein, [^{35}S]r-eag binding was markedly decreased. No [^{35}S]r-eag binding was observed with ^{Mal}r-eag$^{918–937}$. Also, [^{35}S]r-eag$^{191–962}$ binding to ^{Mal}r-eag$^{650–929}$ was markedly decreased in comparison with ^{Mal}r-eag$^{650–937}$ (Figure 4C). Thus, a relatively small carboxy-terminal domain (residues 897–937) was import-

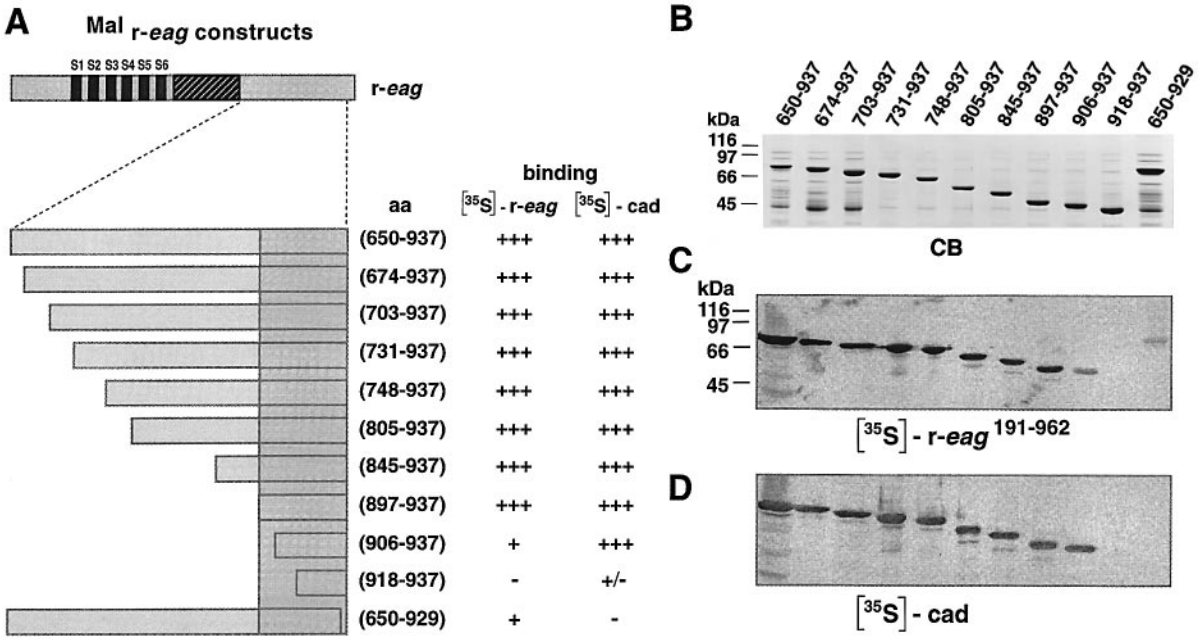

Fig. 4. Interaction of carboxy-terminal r-eag fragments with ^{35}S-labelled r-eag$^{191–962}$ and ^{35}S-labelled cad. (**A**) Diagram illustrating fusion protein constructs between maltose binding protein and carboxy-terminal r-eag fragments (^{Mal}r-eag). Numbers for first and last r-eag residues (aa) in the fusion proteins are given on the right. Full-length r-eag protein is shown on top, as in Figure 3A. Shaded area (residues 897–937) indicates carboxy-terminal r-eag binding region. (**B**) Coomassie blue-stained polyacrylamide gel (CB) of lysates from *E.coli* expressing the ^{Mal}r-eag fusion proteins shown in (A), lane 1 (^{Mal}r-eag$^{650–937}$) corresponds to lane 5 in Figure 3A. The r-eag residues within the constructs are indicated on top of each lane, positions of molecular weight markers (kDa) on the left. Blots of equivalent gels were overlaid with *in vitro*-translated [^{35}S]r-eag$^{191–962}$ (**C**) and [^{35}S]r-eag$^{897–937}$ (cad) (**D**). Bound peptides were visualized by autoradiography. [^{35}S]r-eag$^{191–962}$ and [^{35}S]cad binding results have been evaluated according to the signal intensities obtained in the overlay assays shown in C and D. +++, very strong signal intensity; ±, very weak binding; –, no detectable binding. Evaluations are given next to each ^{Mal}r-eag fusion protein in (A).

ant for r-eag subunit interaction in the overlay binding assays. In contrast, Shaker-related Kv channels contain an amino-terminal subunit interaction domain (Li *et al.*, 1992; Shen *et al.*, 1993; Shen and Pfaffinger, 1995). Since r-eag subunit interaction apparently differs completely from that of Kv channels, we propose to refer to this domain as cad (Carboxy-terminal Assembly Domain).

When we used the cad-sequence ([^{35}S]cad) as probe in the overlay-binding experiments (Figure 4D), [^{35}S]cad and [^{35}S]r-eag binding results to ^{Mal}r-eag$^{650–937}$ were similar. However, [^{35}S]cad and [^{35}S]r-eag binding to ^{Mal}r-eag$^{906–937}$, ^{Mal}r-eag$^{918–937}$ and ^{Mal}r-eag$^{650–929}$ showed interesting differences (summarized in Figure 4A). Unlike [^{35}S]r-eag, [^{35}S]cad bound equally well to ^{Mal}r-eag$^{897–937}$ and ^{Mal}r-eag$^{906–937}$ and bound weakly to ^{Mal}r-eag$^{918–937}$ in the overlay binding assays (Figure 4D). Also, in contrast to [^{35}S]r-eag, [^{35}S]cad binding to ^{Mal}r-eag$^{650–929}$ was not detectable. Apparently, [^{35}S]cad binding was less sensitive than [^{35}S]r-eag to deletions at the amino-terminal cad side and more sensitive than [^{35}S]r-eag to deletions at the carboxy-terminal cad side.

Two subdomains in carboxy-terminal r-eag assembly domain

Alignment of the *Drosophila* (D-eag) (Warmke *et al.*, 1991; Brüggemann *et al.*, 1993) and r-eag cad sequences showed that 12 out of 41 amino acid residues are identical and 18 are conservatively substituted (Figure 5). Since ^{35}S-labelled D-eag probes interacted with the r-eag cad region in overlay binding assays (data not shown), it is most likely that conserved cad amino-acid residues are involved in cad/cad interaction and thus, in r-eag subunit

```
D-eag     918 ATVLDMKVDVRLELQRMQQRIGRIEDLLGELVKRLAPGASS 948 [35S] - r-eag 191-962
r-eag     897 ATVLEVKHELKEDIKALNAKMTSIEKQLSELLRILMSRGSS 937      binding

VEL/AQA     .....A..QA.................................      +
V902A       .....A.....................................      +
E905Q       ........Q..................................      ++
V906A       .........A................................      +
n901-911    ....Q...Q..QQ.Q............................      +
h900-910    ...A.A...A...A.............................      +/-
E921Q E926Q .........................Q....Q...........      +++
E921K E926Q .........................K....Q...........      ++
L929A L931A ...............................A..A......      +++
```

Fig. 5. Influence of point mutations on r-eag subunit interaction. Alignment of *Drosophila* (D)-eag (residues 918–948) and rat (r)-eag (residues 897–937) cad sequences is shown. Identical residues are shaded, similar residues are boxed. Point mutations indicated below were introduced into ^{Mal}r-eag$^{650–962}$. Naming of mutants is given at left. Mutant fusion proteins were tested in overlay binding assays with [^{35}S]r-eag$^{191–962}$ (not shown). Binding results (classified as in Figure 4) are shown on the right.

assembly. Some of these amino acid residues were mutated by site-directed *in vitro* mutagenesis of ^{Mal}r-eag$^{650–937}$ expression plasmids. As shown in Figure 5, charged amino acids were replaced by neutral amino acid residues or by residues of opposite charge. Alternatively, hydrophobic amino acids (I, L, V) were substituted with alanine. We did not readily obtain cad single-point mutations, which strongly reduced or diminished [^{35}S]r-eag binding. Therefore, we introduced multiple mutations into cad (Figure 5). Substitution of the four negatively charged amino acid residues E901, E905, E908, D909 and the positively charged lysine K 911 by glutamine (^{Mal}r-eag$^{650–937,n901–911}$) caused a marked reduction in [^{35}S]r-eag binding (Figure 5). Also, the substitution of V902, E905 and L906 by alanine and glutamine, (^{Mal}r-eag$^{650–937,VEL/AQA}$) affected [^{35}S]r-eag binding. The strongest reduction in [^{35}S]r-eag binding was detected when the four hydrophobic residues

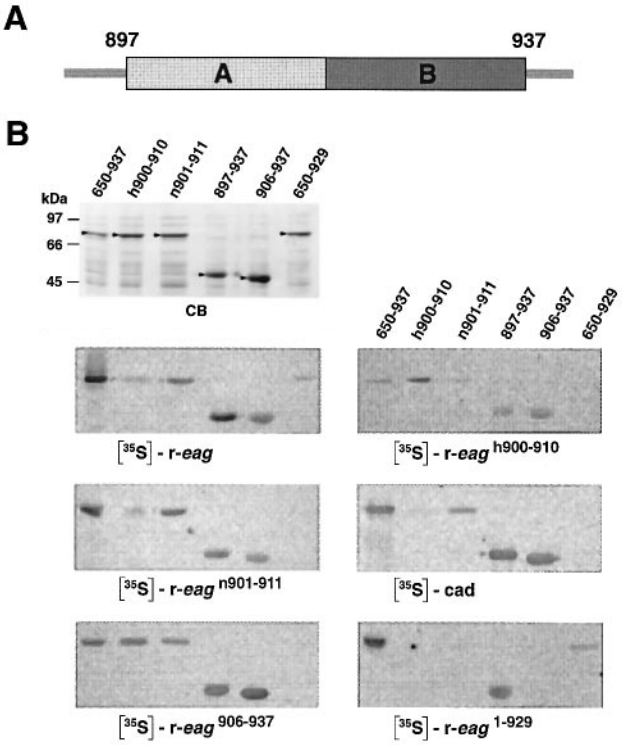

C

		Mal r-eag A+B+		Mal r-eag A-B+			Mal r-eag A+B-
	[35S] - labelled PROBE	650-937	897-937	Mal r-eag h900-910	n901-911	906-937	650-929
AB	[35S] - r-eag	+++	+++	+	++	++	+
	[35S] - cad	++	++	±	+	++	–
B+	[35S] - r-eag h900-910	+	+	++	±	+	–
	[35S] - r-eag n901-911	++	+	+	++	+	–
	[35S] - r-eag 906-937	++	++	++	++	+++	–
A+	[35S] - r-eag 1-929	+++	++	–	–	–	+

Fig. 6. Analysis of cad subdomain interactions. (**A**) Schematic drawing of cad with arbitrary A- and B- subdomain domains. (**B**) Coomassie blue-stained polyacrylamide gel of lysates from *E.coli* expressing Mal fusion proteins with r-eag carboxy-terminus (^{Mal}r-eag$^{650–937}$), r-eag carboxy-terminal point mutations (^{Mal}r-eag$^{650–937;h900–910}$, ^{Mal}r-eag$^{650–937;n901–911}$) or deletion mutants (^{Mal}r-eag$^{897–937}$, ^{Mal}r-eag$^{906–937}$, ^{Mal}r-eag$^{650–929}$) as indicated on top of each lane. Fusion protein bands are marked by arrows. Positions of size markers are given on the left. Blots of equivalent gels were incubated with *in vitro*-translated ^{35}S-labelled r-eag probes as indicated. Bound [^{35}S]r-eag probes were visualized by autoradiography. (**C**) Binding results of the overlay assays in (B) have been evaluated according to the signal intensities as in Figure 4. Fusion protein constructs were sorted as A^-B^+, A^+B^- and A^+B^+ as described in the text. Similarly, [^{35}S]r-eag probes were classified as A^+, B^+ or AB probe, respectively. Shading indicates homotypic A– and B– interactions of cad subdomains.

L900, V902, L906 and I910 had been replaced with alanine (^{Mal}r-eag$^{650–937,h900–910}$). In contrast, mutations, which were introduced in the carboxy-terminal half of cad (E922Q/E926Q; E922K/E926Q; L928A/L931A), did not markedly affect [^{35}S]r-eag binding (Figure 5).

The results suggested that cad function was more sensitive to amino-terminal than carboxy-terminal amino acid substitutions. Also, relatively small deletions from both cad ends affected markedly r-eag subunit assembly. These observations suggested to us that cad might be divided into two subdomains, A and B (Figure 6A). The subdomains could bind to each other either in an A–A, B–B or in an A–B manner. To test these alternatives we examined in the overlay assay various cad-mutants, where either the A or the B subdomain was mutated. The mutants ^{Mal}r-eag$^{650–937,h900–910}$, ^{Mal}r-eag$^{650–937,n901–911}$ and ^{Mal}r-eag$^{906–937}$ were taken as A-subdomain mutants (^{Mal}r-eag$^{A–B+}$ in Figure 6C) and ^{Mal}r-eag$^{650–929}$ as B-subdomain mutant (^{Mal}r-eag$^{A+B–}$ in Figure 6C). Blots of the mutant fusion proteins were probed either with probes containing an intact cad sequence ([^{35}S]r-eag; [^{35}S]cad) ('AB'-probe) or with ones containing a mutated A-subdomain ([^{35}S]r-eag$^{h900–910}$; [^{35}S]r-eag$^{n901–911}$; [^{35}S]r-eag$^{906–937}$) ('B^+' probe) or a mutated B-subdomain ([^{35}S]r-eag$^{1–929}$) ('A^+'-probe), respectively. The results of the overlay binding experiments using the different A, B and AB fusion proteins and probes are shown in Figure 6B. The various A- and B-subdomain mutations had distinct effects on cad-binding as summarized schematically in Figure 6C. The data indicate that the 'A^+'-probe [^{35}S]r-eag$^{1–929}$ bound only to the ^{Mal}r-eag fusion proteins (^{Mal}r-eag$^{650–929}$, ^{Mal}r-eag$^{650–937}$, ^{Mal}r-eag$^{897–937}$) with an intact A-subdomain and did not bind to the ones with a mutated A-subdomain (^{Mal}r-eag$^{h900–910}$, ^{Mal}r-eag$^{n901–911}$, ^{Mal}r-eag$^{906–937}$). Similarly, [^{35}S]r-eag 'B^+'-probes bound only to the ^{Mal}r-eag fusion proteins with an intact B-domain (^{Mal}r-eag$^{h900–910}$, ^{Mal}r-eag$^{n901–911}$, ^{Mal}r-eag$^{906–937}$) and did not bind to the one with a mutated B-domain (^{Mal}r-eag $^{650–929}$). [^{35}S]r-eag, containing both subdomains A and B, bound to ^{Mal}r-eag fusion proteins, regardless of whether they carried a mutated subdomain A or B, respectively. Interestingly, binding of [^{35}S]r-eag$^{1–962,h900–910}$ to the ^{Mal}r-eag$^{650–937,h900–910}$ fusion protein was stronger than binding of [^{35}S]r-eag$^{1–962,h900–910}$ to ^{Mal}r-eag$^{650–937}$. The binding data indicated that the cad-subdomains interact with each other in a homophilic A–A, B–B manner (Figure 6C). This suggested that mutations of both cad A- and B-subdomains are necessary to eliminate completely any r-eag subunit interaction. This supposition was tested in the functional CHO expression system.

Mutant r-eag carboxy-terminus does not suppress r-eag current

Combining the results of the overlay binding assays in Figure 6 and those of r-eag expression in Figure 2 suggested that r-eag$^{1–896}$ (Figure 2D) did not express functional r-eag channels because the cad-domain had been eliminated. On the other hand, expression of carboxy-terminally truncated r-eag$^{1–915}$ with a missing cad B-subdomain produced functional r-eag channels (Figures 2C and 7A). Expression of r-eag subunits with a mutated cad A-subdomain (r-eag$^{h900–910}$) also produced functional r-eag channels (Figure 7B). In contrast, no r-eag currents were detected when we attempted to express r-eag subunits with a mutated cad A- and a missing cad B-subdomain (r-eag$^{1–915,h900–910}$) (n = 7; Figure 7C). Thus, the cad domain is essential for functional r-eag channel expression (Figure 2).

In Figure 1, we showed that the presence of a 10-fold molar excess of r-*eag*$^{650–962}$ mRNA suppressed the expression of r-eag channels by r-*eag* mRNA. By contrast, a 10-fold molar excess of r-*eag*$^{1–896}$ mRNA lacking the

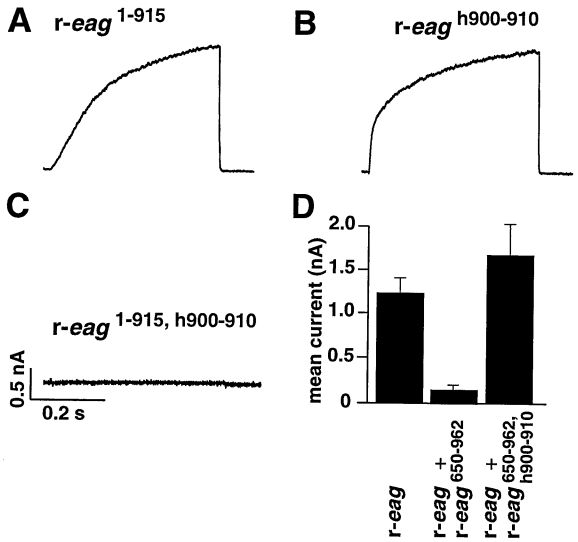

Fig. 7. Effect of carboxy-terminal cad mutations on functional r-eag expression in CHO cells. CHO cells were injected with (**A**) r-*eag*$^{1–915}$, (**B**) r-*eag*$^{h900–910}$ and (**C**) r-*eag*$^{1–915,h900–910}$ mRNA ~6 h before recording using whole-cell patch–clamp method. Conditions as described in Materials and methods. Currents were evoked with voltage jumps to +60 mV from a holding potential of –60 mV. (**D**) Data pooled from a number of experiments in which mRNAs r-*eag*, r-*eag* plus r-*eag*$^{650–962}$ or r-*eag* plus r-*eag*$^{650–962,h900–910}$ mRNAs were injected into CHO cells. Currents were recorded after 4 h and peak amplitudes were measured following a 500 ms voltage step to +60 mV. In each case the histogram represents the mean of measurements from between four and 18 different cells, and the vertical bars the SEM.

cad-domain did not abolish the expression of r-eag channels by r-*eag* mRNA (data not shown). The dominant-negative effect of the r-eag$^{650–692}$ carboxy-terminus on functional r-eag channel expression was most likely due to an interference with the assembly of r-eag subunits. Accordingly, r-eag carboxy-termini with a mutant cad domain should not be able to interfere with functional r-eag channel expression. Indeed, normal r-eag outward currents were recorded with a mean amplitude at +60 mV of 1.65 ± 0.35 nA (n = 4; Figure 7D) when r-*eag* mRNA was co-expressed in CHO cells with a 10-fold molar excess of r-*eag*$^{650–962,h900–910}$ mRNA,. Similar results were obtained, when r-*eag* mRNA was co-expressed with a 10-fold molar excess of r-*eag*$^{650–962,VEL/AQA}$ mRNA (1.19 ± 0.4 nA at +60 mV; n = 3). The results show that cad mutations abolished the dominant-negative effect of the r-eag$^{650–962}$ carboxy-terminus on functional r-eag channel expression. Thus, the *in vitro* expression studies with mutant cads confirmed the important role of cad in r-eag subunit assembly.

Discussion

In the present study we have investigated the subunit assembly requirements of r-eag, a member of the eag family of voltage-gated K-channels (Warmke *et al.*, 1991; Ludwig *et al.*, 1994; Warmke and Ganetzky, 1994) using the complementary methods of protein binding (overlay assay) and functional expression of r-eag channels (mRNA injection into CHO cells and whole-cell patch–clamp). Our results show that assembly of r-eag channels involves a carboxy-terminal domain (cad). The principal evidence for this conclusion is drawn from a number of observations: (i) in protein–protein overlay assays, ^{35}S-labelled r-eag binds to fusion proteins carrying the carboxy-terminus and not to fusion protein carrying the amino-terminus; (ii) injections of subunits truncated from the carboxy-terminus beyond residue 896 do not result in the expression of functional channels; (iii) the carboxy-terminus r-eag (r-eag$^{650–962}$), but not the amino-terminus of r-eag (r-eag$^{1–208}$), exerted a dominant-negative effect on r-eag channel expression; and (iv) cad-mutations affect functional r-eag channel expression as well as the dominant-negative effect of co-expressed r-eag carboxy-terminus on r-eag currents.

Alternative explanations for the failure of the mRNAs which encoded r-eag mutants to produce functional channels when injected into CHO cells might be: (i) the inability of the cell to transport the protein to the plasma membrane; (ii) improper folding of the peptide chain; and (iii) loss of post-translational modifications necessary for channel function. However, these reasons are unlikely in the case of the dominant-negative effect of the carboxy-terminus since the amino-terminus does not have this effect on r-eag and neither the carboxy- nor amino-terminus has any such effect on the Kv1.5 channel expressed in the same system. Furthermore, the overlay assay gives a direct indication of binding between proteins in a cell-free system and is therefore not subject to the above considerations.

Using the overlay binding assay we have defined a minimal region (cad) for homophilic r-eag subunit interactions in the r-eag carboxy-terminus (residues 897–937). The cad peptide is the shortest peptide in the overlay assay that is bound at the apparent same intensity as the complete carboxy-terminus by the full-length r-eag protein. Cad is also bound strongly by itself, suggesting that important elements for assembly of subunits are contained within this region. Consistent with this idea are the observations that r-eag subunits lacking a functional cad (e.g. ^{Mal}r-eag$^{1–896}$; ^{Mal}r-eag$^{1–915,h900–910}$) did not express r-eag channels and that mutations of cad residues (e.g. ^{Mal}r-eag$^{650–937,h900–910}$) could dramatically alter binding to [^{35}S]r-eag in the overlay assay and also abolish the dominant-negative effect seen previously with r-eag$^{650–962}$ in the co-expression assay.

A mutational analysis of cad suggests that it may consist of two subdomains, A and B. The A subdomain probably resides between residues 897–917, the B subdomain between residues 918–937. In both the overlay binding and the functional expression assays it was apparently necessary to mutate and/or delete both cad subdomains to eliminate the cad/cad binding reaction and r-eag channel expression, respectively. The major conclusion from these results was that the cad subdomains bound to each other in a homophilic manner, i.e. subdomain A bound to probes containing subdomain A, and subdomain B bound to probes containing subdomain B, whereas subdomain A/subdomain B interactions did not take place. We observed, however, an apparent inconsistency with this proposition when we used ^{35}S-labelled cad probes. This probe did not bind to fusion proteins lacking subdomain B (e.g. ^{Mal}r-eag$^{650–929}$), but appeared to bind to fusion proteins lacking subdomain A (^{Mal}r-eag$^{906–937}$), with the same

intensity as to fusion protein containing a complete cad (^{Mal}r-eag$^{650–962}$). It suggests that additional sequences within the r-eag carboxy-terminus between residues 650 and 937 are necessary to maintain proper folding of the cad, and in particular that of subdomain A. This observation may explain why co-expression of cad peptide and r-eag subunits did not inhibit r-eag channel expression in contrast to the co-expression of r-eag and r-eag$^{650–962}$ carboxy-terminus. Alternatively, we may have missed in our analysis an additional r-eag domain within the r-eag$^{650–937}$ carboxy-terminus that is necessary for r-eag subunit assembly. The fact that such regions could not be identified using the overlay assay might be due to a shortcoming of this experimental approach. The affinity of additional assembly domain(s) to their binding partners might be either too low to be seen in the overlay assay or depend on folding processes that do not occur with immobilized r-eag protein.

Our results show that the cad subdomains associate through a homophilic A–A, B–B interaction (Figure 6). This association in principle could be sufficient for channel assembly. It might, however, be expected from this proposition that a loss of subdomain A or subdomain B function should prevent the assembly of r-eag subunits to functional r-eag channels. Yet r-eag subunits with a mutant subdomain A (r-eag$^{1–962,h900–910}$) or with a mutant subdomain B (r-eag$^{1–915}$) were able in the CHO expression system to form channels mediating r-eag outward currents. Functional expression was only lost when both subdomains' mutations were combined, as in r-eag$^{1–915,h900–910}$. A possible interpretation of these results is that the homophilic subdomain interactions led to the formation of r-eag dimers. The dimerization may induce a conformational change and create new subunit interfaces being involved in the final tetramerization step. This type of subunit assembly might have gone undetected in the overlay binding assays. On the other hand, the residual interactions between mutated cads might still have been sufficient to direct functional expression of r-eag channels in the CHO expression system. Alternatively, other parts of the polypeptide chain might comprise additional assembly domains. The affinity of this putative domain(s) to their partners might either be too low to be seen in the overlay assay or depend on folding processes that do not occur with immobilized protein.

For another member of the eag family, the human *ether-à-go-go*-related gene encoded K-channel (HERG), Li *et al.* (1997) have recently described an amino-terminal domain that is capable of self-tetramerization. Co-expression of the corresponding mRNA with HERG mRNA led to a small reduction in HERG-mediated currents in transfected cells. However, Schönherr and Heinemann (1996) and Spector *et al.* (1996) demonstrated that amino-terminal HERG deletion mutants (Δ2–373 and Δ2–354, respectively) which were missing almost the complete cytoplasmic amino-terminal domain in front of S1, still formed functional channels in the *Xenopus* expression system, indicating that the HERG amino-terminus is not essential for HERG-channel expression. The importance of the HERG carboxy-terminus for HERG-subunit assembly has not yet been studied.

Previously, the assembly of Shaker-related Kv-channels has been studied using similar approaches as described for r-eag in this paper (Li *et al.*, 1992; Shen *et al.*, 1993; Shen and Pfaffinger, 1995). In contrast to our findings with r-eag, it was shown that the Kv channel subunits possess an amino-terminal assembly or tetramerization T-domain which by itself is capable of forming tetramers (Pfaffinger and De Rubeis, 1995). Also, in co-expression studies the T-domain exerts a dominant-negative effect on Kv channel expression like the r-eag carboxy-terminal cad on r-eag channel expression. Furthermore, the T-domain is subdivided into subdomains. How these subdomains interact with each other is, however, not known. The presence of a functional T-domain may not be absolutely required for Kv channel expression in the *Xenopus* oocyte expression system (Tu *et al.*, 1996). Other interactions, presumably between the hydrophobic domains, might also contribute to the assembly of K channels. Evidence that such interactions contribute to the assembly of inward rectifier K channels has been provided by Tucker *et al.* (1996). Similarly, Peled-Zehavi *et al.* (1996) have shown for Kv channels that the S3 region can associate with S4, and likewise S3 and S4 can interact with S2 when the respective peptides have been inserted into artificial lipid bilayers. Possibly, the amino-terminal T-domain of Kv channels primarily controls the specificity of Kv α-subunit assembly as well as that with Kv β-subunits (Sewing *et al.*, 1996; Yu *et al.*, 1996). In fact, Lee *et al.* (1994) have shown that it is indeed possible to obtain functional heteromultimeric Kv channels composed of subunits from different families if the entire amino-terminus with the T-domain is deleted. It remains to be shown whether cad might function similarly for eag channels, i.e. directing the specificity of subunits interactions. In any case, the expression data demonstrate that the cad-containing r-eag carboxy-terminus is required for functional r-eag channel expression, whereas the amino-terminus apparently is not (Terlau *et al.*, 1997).

It has been previously proposed that, in *Drosophila*, the eag protein may represent a subunit common to different types of K channels (Wu *et al.*, 1983; Zhong and Wu, 1991, 1993). Evidence has recently been presented in support of the possibility that eag subunits can form heteromultimers with Shaker subunits (Chen *et al.*, 1996). In the present study we have not specifically addressed this question. However, our finding that co-expression of r-eag carboxy- or amino-termini with Shaker-type Kv1.5 subunits is without effect on Kv1.5 channel expression, does not support this idea.

Materials and methods

Molecular biology and cloning

mRNAs were prepared from *Not*I-linearized r-*eag* wild-type or mutant constructs in pGEMHE (a gift of P.Tytgat, Leuven) using an AMBION T7 m-message machine kit according to the manufacturer's instructions.

Amino-terminus deletion mutants were constructed using PCR with primers that carried a *Bam*HI enzyme recognition site, a ribosomal binding site (Kozak, 1986) and a translation initiation codon followed by 15–20 bases of the desired r-eag coding sequence. Carboxy-terminus deletion mutants were constructed using antisense primers carrying a *Hin*dIII recognition site, a termination codon and 15–20 nucleotides of the r-*eag* sequence. The PCR fragments were then reinserted in the appropriate plasmids carrying r-*eag* cDNA. Point mutations were introduced in fragments of the coding region using a PCR-based overlap–extension method (Ho *et al.*, 1989) and reinserted into the original clone using appropriate restriction enzymes. All constructs were sequenced

using the dideoxy chain termination method (Sanger *et al.*, 1977) with double-stranded plasmid DNA as template to ensure absence of polymerase errors.

For expression in *E.coli*, r-*eag* cDNAs (wild-type and mutant constructs) were cloned into the *Bam*HI and *Hin*dIII restriction sites of a pMAl 2c vector (NEB). The lacI^q gene was inactivated by restriction with *Bsp*120I, filled in with T4 DNA polymerase and subsequent religation, thus leading to plasmids constitutively expressing r-eag constructs as maltose binding protein (Mal) fusion proteins.

Nomenclature of constructs

r-eag deletion mutants are designated as r-eag$^{xxx–yyy}$, where xxx and yyy indicate the first and last r-eag residue, respectively. Initiating methionines were additionally introduced. Point mutations are indicated as AxxxB where B designates the amino acid that replaced amino acid A at position xxx. Maltose binding protein fusion constructs are indicated by the superscript ^{Mal}.

Overexpression

Escerichia coli Xl1blue cells were transformed with expression constructs and grown overnight at 37°C. Cells were harvested by centrifugation and lysed in Läemmli buffer at 56°C.

In vitro translation and overlay experiments

^{35}S-labelled probes and proteins were synthesized from the respective mRNAs by *in vitro* translation in the Flexi rabbit reticulocyte lysate system (Promega). Mal fusion proteins in total *E.coli* lysates were separated by 7.5% or 9% SDS–polyacrylamide gel electrophoresis (SDS–PAGE). For visualization of protein bands, gels were stained with Coomassie blue. For overlays, the gels were blotted onto nitrocellulose and blocked with 5% non-fat dry milk and 1% L-methionine in phosphate-buffered saline (PBS). Blots were incubated with translation reaction in overlay buffer [5% bovine serum albumin (BSA), 1% L-methionine, 0.5% non-fat dry milk in PBS; 5–25 µl of *in vitro* translation reaction product per ml of buffer] with gentle mixing for 3–6 h at room temperature, washed for 2×20 min in 5% BSA, 1% L-methionine in PBS, air-dried and exposed for 4–16 h to phosphor-imaging plates. The plates were scanned with Fuji X-Bas 2000 phosphor-imager.

Cell culture and mRNA injection

A dihydrofolate reductase-lacking subclone of the Chinese hamster ovary cell-line (CHO-*dhfr*$^-$) was cultured according to standard methods at 37°C and 5% CO_2. The growth medium was based on MEM-α with nucleosides (Gibco). When cells were confluent, they were split and plated at low density [2–3 cells per 175 µm grid (CelLocates: Eppendorf)]. After ~12 h, cells were microinjected with solutions containing ~50 ng/ml mRNA for various proteins including r-eag (wt), mutant r-eag subunits, rKv1.5 and green fluorescent protein (GFP) after Ikeda *et al.* (1992). For co-expression experiments, mRNA encoding different fragments of r-eag were mixed with either r-*eag* wt or rKv1.5 wt RNA, respectively, to give the approximate molar ratios of RNA as stated in Results.

Electrophysiological recordings

Electrophysiological recordings were made between 4 and 8 h after mRNA injection, using the whole-cell patch–clamp method. Patch pipettes were pulled from borosilicate capillaries (1.5 mm OD; Clark Electromedical, UK) using a DMZ Universal Puller (Zeitz, Germany) and fire-polished on the puller. The electrodes had resistances of ~4.5 MΩ when filled with the intracellular solution consisting of 145 mM K-aspartate, 30 mM KCl, 11 mM EGTA, 1 mM $CaCl_2$, 3 mM $MgCl_2$, 10 mM HEPES, pH 7.2. The external bathing solution consisted of 140 mM NaCl, 2.5 mM KCl, 2 mM $CaCl_2$, 2 mM $MgCl_2$, 10 mM HEPES, 10 mM glucose, 20 mM sucrose, pH 7.4.

Recordings were made using an EPC-9 patch–clamp amplifier in conjunction with a Macintosh Power PC (8100/80) and the data acquisition and amplifier control program, Pulse+PulseFit (HEKA, Germany). Data were analysed using PulseFit (HEKA) and IGOR (Wavemetrics Inc., USA). Currents were routinely activated from a holding potential of –60 mV and always included a standard pulse to +60 mV (500 ms duration) at which measurements of currents resulting from injection of cRNA subsequently were made for comparison. Currents were sampled at 100 µs per point and filtered at 3 kHz. The peak current at the end of the voltage step was measured in all cases. Data are given as mean ± SEM. In most cases the threshold for activation was also determined, using series of depolarizing voltage steps, and voltage-dependent slowing of activation was tested (for comparison, conditioning potentials of −20 mV and −110 mV), these being characteristic features of the wild-type r-eag current. A P/4 method of leak subtraction (Pulse+Pulsefit, HEKA) was routinely applied and series resistance compensation of ⩾60% was also applied with currents >1 nA. The estimated error in clamp potential was between 3 and 5 mV.

Acknowledgements

The authors thank C.Schmidt for excellent technical assistance and D.Clausen for help with the figures. O.P. thanks the Deutsche Forschungsgemeinschaft and the Fonds der Chem. Industrie for support.

References

Anderson,J.A., Huprikar,S.S., Kochian,L.V., Lucas,W.J. and Gaber,R.F. (1992) Functional expression of a probable *Arabidopsis thaliana* potassium channel in *Saccharomyces cerevisiae*. *Proc. Natl Acad. Sci. USA*, **89**, 3736–3740.

Brüggemann,A., Pardo,L.A., Stühmer,W. and Pongs,O. (1993) *Ether-à-go-go* encodes a voltage-gated channel permeable to K^+ and Ca^{2+} and modulated by cAMP. *Nature*, **365**, 445–448.

Chen,M.L., Hoshi,T. and Wu,C.F. (1996) Heteromultimeric interactions among K^+ channel subunits from *Shaker* and *eag* families in *Xenopus* oocytes. *Neuron*, **17**, 535–542.

Deal,K.K., Lovinger,D.M and Tamkun,M.M. (1994) The brain Kv1.1 potassium channel: *in vitro* and *in vivo* studies on subunit assembly and posttranslational processing. *J. Neurosci*., **14**, 1666–1676.

Hille,B. (1992) *Ionic Channels of Excitable Membranes*. Second edn. Sinauer Associates, Inc., Sunderland, Massachusetts.

Ho,S.N., Hunt,H.D., Horton,R.M., Pullen,J.K. and Pease,L.R. (1989) Site-directed mutagenesis by overlap extension using the polymerase chain reaction. *Gene*, **77**, 51–59.

Hopkins,W.F., Demas,V. and Tempel,B.L. (1994) Both N- and C-terminal regions contribute to the assembly and functional expression of homo- and heteromultimeric voltage-gated K^+ channels. *J. Neurosci*., **14**, 1385–1393.

Ikeda,S.R., Soler,F., Zuhlke,R.D., Joho,R.H. and Lewis,D.L. (1992) Heterologous expression of the human potassium channel Kv2.1 in clonal mammalian cells by direct cytoplasmic microinjection of cRNA. *Pflügers Arch*., **422**, 201–203.

Kaupp,U.B. *et al*. (1989) Primary structure and functional expression from complementary DNA of the rod photoreceptor cyclic GMP-gated channel. *Nature*, **342**, 762–766.

Kozak,M. (1986) Point mutations define a sequence flanking the AUG initiator codon that modulates translation by eukaryotic ribosomes. *Cell*, **44**, 283–292.

Lee,T.E., Philipson,L.H., Kuznetsov,A. and Nelson,D.J. (1994) Structural determinant for assembly of mammalian K^+ channels. *Biophys. J*., **66**, 667–673.

Li,M., Jan,Y.N. and Jan,L.Y. (1992) Specification of subunit assembly by the hydrophilic amino-terminal domain of the *Shaker* potassium channel. *Science*, **257**, 1225–1230.

Li,X., Xu,J. and Li,M. (1997) The human Δ1261 mutation of the *HERG* potassium channel results in a truncated protein that contains a subunit interaction domain and decreases the channel expression. *J. Biol. Chem*., **272**, 705–708.

Liman,E.R., Tytgat,J. and Hess,P. (1992) Subunit stoichiometry of a mammalian K^+ channel determined by construction of multimeric cDNAs. *Neuron*, **9**, 861–871.

Liu,D.T., Tibbs,G.R. and Siegelbaum,S.A. (1996) Subunit stoichiometry of cyclic nucleotide-gated channels and effects of subunit order on channel function. *Neuron*, **16**, 983–990.

Ludwig,J., Terlau,H., Wunder,F., Brüggemann,A., Pardo,L.A., Marquardt,A., Stühmer,W. and Pongs,O. (1994) Functional expression of a rat homologue of the voltage gated *ether-à-go-go* potassium channel reveals differences in selectivity and activation kinetics between the *Drosophila* channel and its mammalian counterpart. *EMBO J*., **13**, 4451–4458.

MacKinnon,R. (1991) Determination of the subunit stoichiometry of a voltage-activated potassium channel. *Nature*, **350**, 232–235.

Parcej,D.N. and Dolly,J.O. (1989) Dendrotoxin receptor from bovine synaptic plasma membranes. Binding properties, purification and subunit composition of a putative constituent of certain voltage-activated K^+ channels. *Biochem. J*., **257**, 899–903.

Parcej,D.N., Scott,V.E.S. and Dolly,J.O. (1992) Oligomeric properties of α-dendrotoxin-sensitive potassium ion channels purified from bovine brain. *Biochemistry*, **31**, 11084–11088.

Peled-Zehavi,H., Arkin,I.T., Engelman,D.M. and Shai,Y. (1996) Coassembly of synthetic segments of *Shaker* K^+ channel within phospholipid membranes. *Biochemistry*, **35**, 6828–6838.

Pfaffinger,P.J. and DeRubeis,D. (1995) *Shaker* K^+ channel T1 domain self-tetramerizes to stable structure. *J. Biol. Chem.*, **270**, 28595–28600.

Rehm,H. and Lazdunski,M. (1988) Purification and subunit structure of a putative K^+ channel protein identified by its binding properties for dendrotoxin I. *Proc. Natl Acad. Sci. USA*, **85**, 4919–4923.

Rettig,J., Heinemann,S.H., Wunder,F., Lorra,C., Parcej,D.N., Dolly,O. and Pongs,O. (1994) Inactivation of voltage-gated K^+ channels altered by presence of β-subunits. *Nature*, **369**, 289–294.

Sanger,F., Nicklen,S. and Coulson,A.R. (1977) DNA sequencing with chain-terminating inhibitors. *Proc. Natl Acad. Sci. USA*, **74**, 5463–5467.

Schönherr,R. and Heinemann,S.H. (1996) Molecular determinants for activation and inactivation of HERG, a human inward rectifier potassium channel. *J. Physiol.*, **493**, 635–642.

Sentenac,H., Bonneaud,N., Minet,M., Lacroute,F., Salmon,D.M., Gaymard,F. and Grignon,C. (1992) Cloning and expression in yeast of a plant potassium ion transport system. *Science*, **256**, 663–665.

Sewing,S., Röper,J. and Pongs,O. (1996) Kvβ1 subunit binding specific for *Shaker*-related potassium channel α subunits. *Neuron*, **16**, 455–463.

Shen,N.V. and Pfaffinger,P.J. (1995) Molecular recognition and assembly sequences involved in the subfamily-specific assembly of voltage-gated K^+ channel subunit proteins. *Neuron*, **14**, 625–633.

Shen,N.V., Chen,X., Boyer,M.M. and Pfaffinger,P.J. (1993) Deletion analysis of K^+ channel assembly. *Neuron*, **11**, 67–76.

Spector,P.S., Curran,M.E., Zou,A., Keating,M.T. and Sanguinetti,M.C. (1996) Fast inactivation causes rectification of the I_{Kr} channel. *J. Gen. Physiol.*, **107**, 611–619.

Stansfeld,C.E., Röper,J., Ludwig,J., Weseloh,R.M., Marsh,S.J., Brown, D.A. and Pongs,O. (1996) Elevation of intracellular calcium by muscarinic receptor activation induces a block of voltage-activated rat *ether-à-go-go* channels in a stably transfected cell line. *Proc. Natl Acad. Sci. USA*, **93**, 9910–9914.

Terlau,H., Ludwig,J., Steffan,R., Pongs,O., Stühmer,W. and Heinemann, S.H. (1996) Extracellular Mg^{2+} regulates activation of rat *eag* potassium channel. *Pflügers Arch.*, **432**, 301–312.

Terlau,H., Heinemann,S.H., Stühmer,W., Pongs,O. and Ludwig,J. (1997) Amino terminal dependent gating of the potassium channel rat *eag* is compensated by mutation in S4. *J. Physiol.*, **502**, **3**, 537–543.

Tu,L.W., Santarelli,V., Sheng,Z.F., Skach,W., Pain,D. and Deutsch,C. (1996) Voltage-gated K^+ channels contain multiple intersubunit association sites. *J. Biol. Chem.*, **271**, 18904–18911.

Tucker,S.J., Bond,C.T., Herson,P., Pessia,M. and Adelman,J.P. (1996) Inhibitory interactions between two inward rectifier K^+ channel subunits mediated by the transmembrane domains. *J. Biol. Chem.*, **271**, 5866–5870.

Warmke,J.W. and Ganetzky,B. (1994) A family of potassium channel genes related to *eag* in *Drosophila* and mammals. *Proc. Natl Acad. Sci. USA*, **91**, 3438–3442.

Warmke,J., Drysdale,R. and Ganetzky,B. (1991) A distinct potassium channel polypeptide encoded by the *Drosophila eag* locus. *Science*, **252**, 1560–1562.

Wu,C.F., Ganetzky,B., Haugland,F.N. and Liu,A.X. (1983) Potassium currents in *Drosophila*: different components affected by mutations of two genes. *Sciences*, **220**, 1076–1078.

Xu,J., Yu,W., Jan,Y.N., Jan,L.Y. and Li,M. (1995) Assembly of voltage-gated potassium channels: conserved hydrophilic motifs determine subfamily-specific interactions between the α-subunits. *J. Biol. Chem.*, **270**, 24761–24768.

Yu,W., Xu,J. and Li,M. (1996) NAB domain is essential for the subunit assembly of both α-α and α-β complexes of *Shaker*-like potassium channels. *Neuron*, **16**, 441–453.

Zhong,Y. and Wu,C.F. (1991) Alteration of four identified K^+ currents in *Drosophila* muscle by mutations in *eag*. *Science*, **252**, 1562–1564.

Zhong,Y. and Wu,C.F. (1993) Modulation of different K^+ currents in *Drosophila*: a hypothetical role for the *eag* subunit in multimeric K^+ channels. *J. Neurosci.*, **13**, 4669–4679.

Received on May 26, 1997; revised on July 22, 1997